

Inspiraling streams of enriched gas observed around a massive galaxy 11 billion years ago

Shiwu Zhang^{1†}, Zheng Cai^{1,2*†}, Dandan Xu¹, Rhythm Shimakawa^{3,4}, Fabrizio Arrigoni Battaia⁵, Jason Xavier Prochaska^{6,7}, Renyue Cen^{8,9}, Zheng Zheng¹⁰, Yunjing Wu¹, Qiong Li^{11,12}, Liming Dou¹³, Jianfeng Wu¹⁴, Ann Zabludoff¹⁵, Xiaohui Fan¹⁵, Yanli Ai¹⁶, Emmet Gabriel Golden-Marx¹, Miao Li¹⁷, Youjun Lu^{18,19}, Xiangcheng Ma²⁰, Sen Wang¹, Ran Wang¹¹, Feng Yuan²¹

Stars form in galaxies, from gas that has been accreted from the intergalactic medium. Simulations have shown that recycling of gas—the reaccretion of gas that was previously ejected from a galaxy—could sustain star formation in the early Universe. We observe the gas surrounding a massive galaxy at redshift 2.3 and detect emission lines from neutral hydrogen, helium, and ionized carbon that extend 100 kiloparsecs from the galaxy. The kinematics of this circumgalactic gas is consistent with an inspiraling stream. The carbon abundance indicates that the gas had already been enriched with elements heavier than helium, previously ejected from a galaxy. We interpret the results as evidence of gas recycling during high-redshift galaxy assembly.

Refs:

- Cai et al. (2016), ApJ, 833, 135
Cai et al. (2017a), ApJ, 837, 71
Cai et al. (2017b), ApJ, 839, 131

Arrigoni Battaia,...,Z.C., et al., A&A, 620, A202
Emonts, Z.C., et al., (2019), ApJ, 887, 86
Li, ..., Z.C., et al., (2021), 922, 236

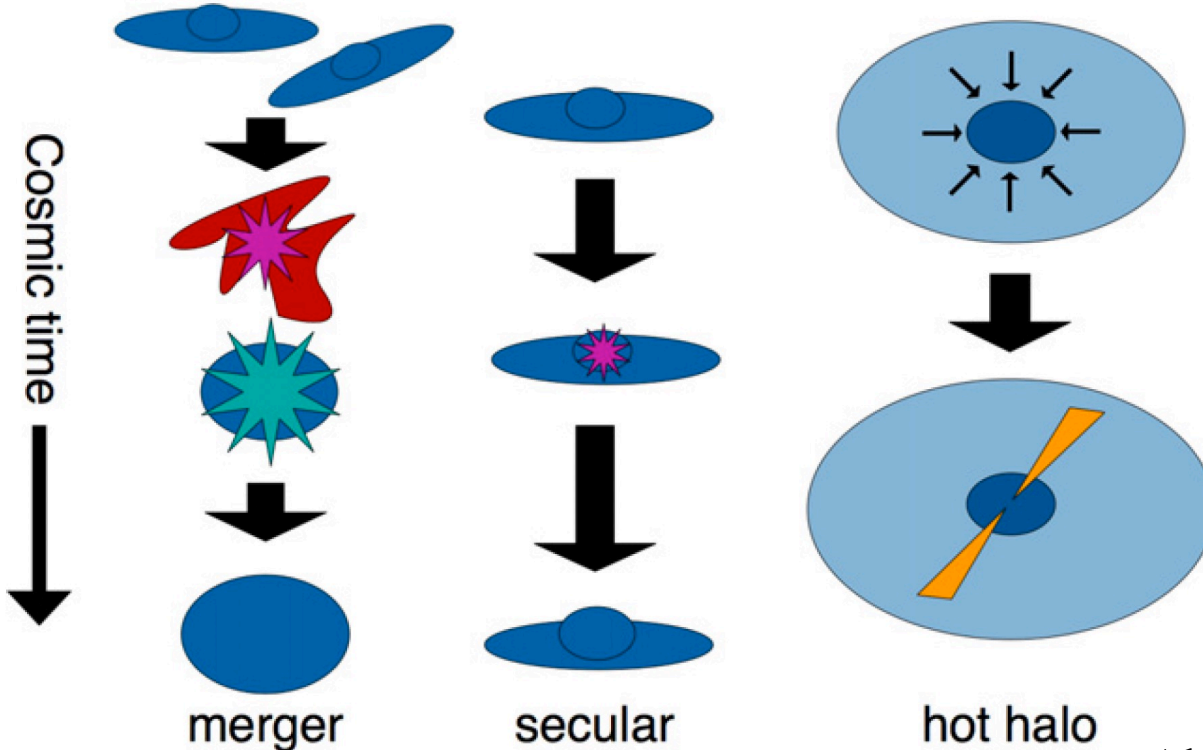
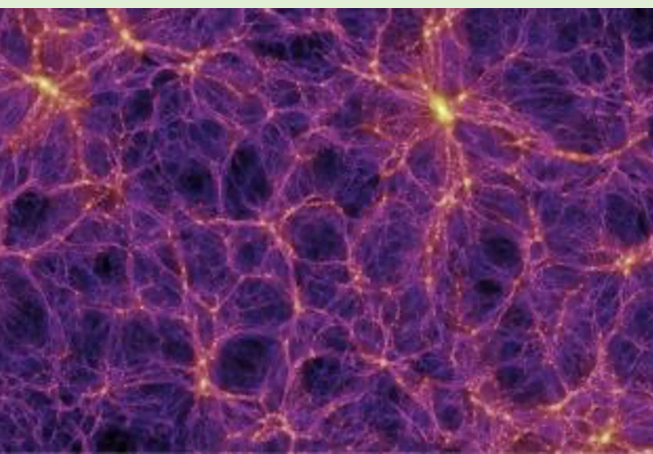
SMBH \rightarrow host galaxy (ISM) \rightarrow CGM \rightleftharpoons LSS (IGM)

0.1 pc

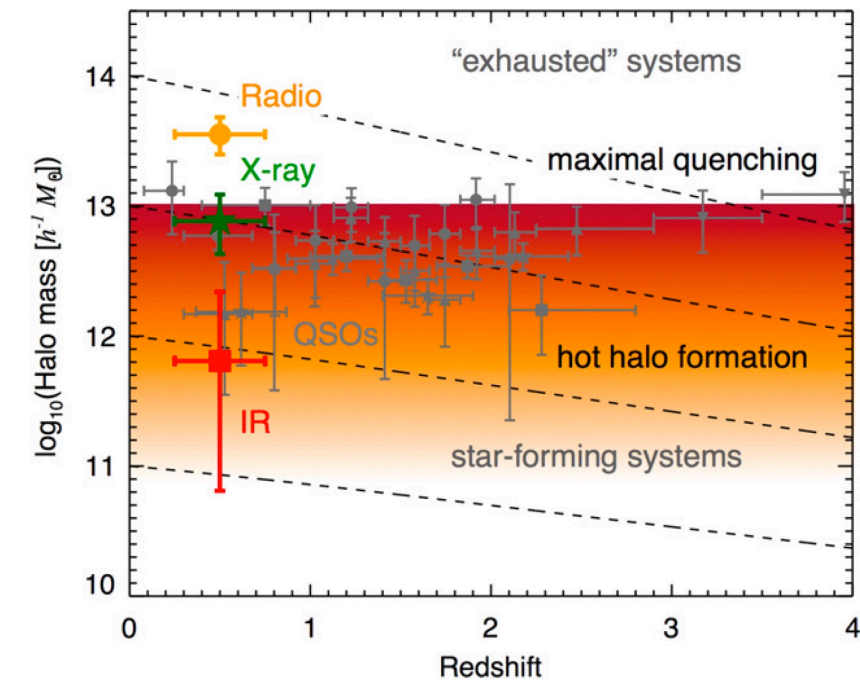
10 kpc

150 kpc

10 Mpc

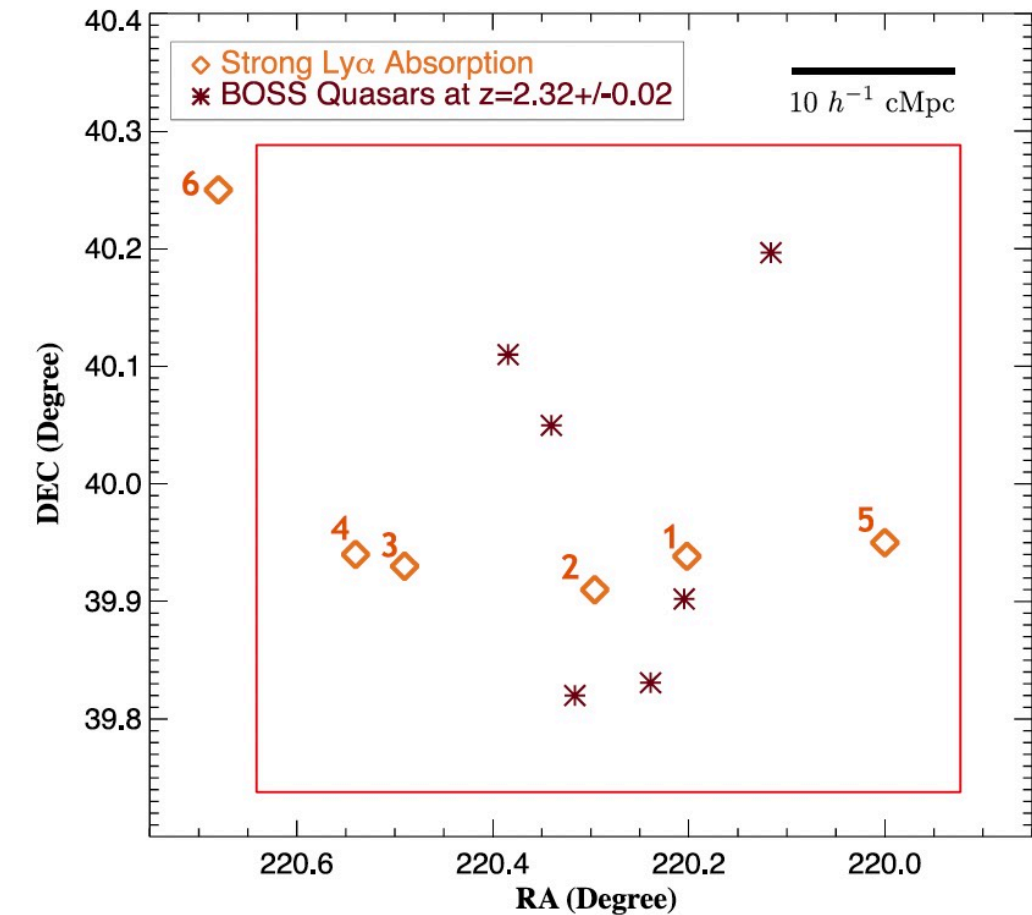
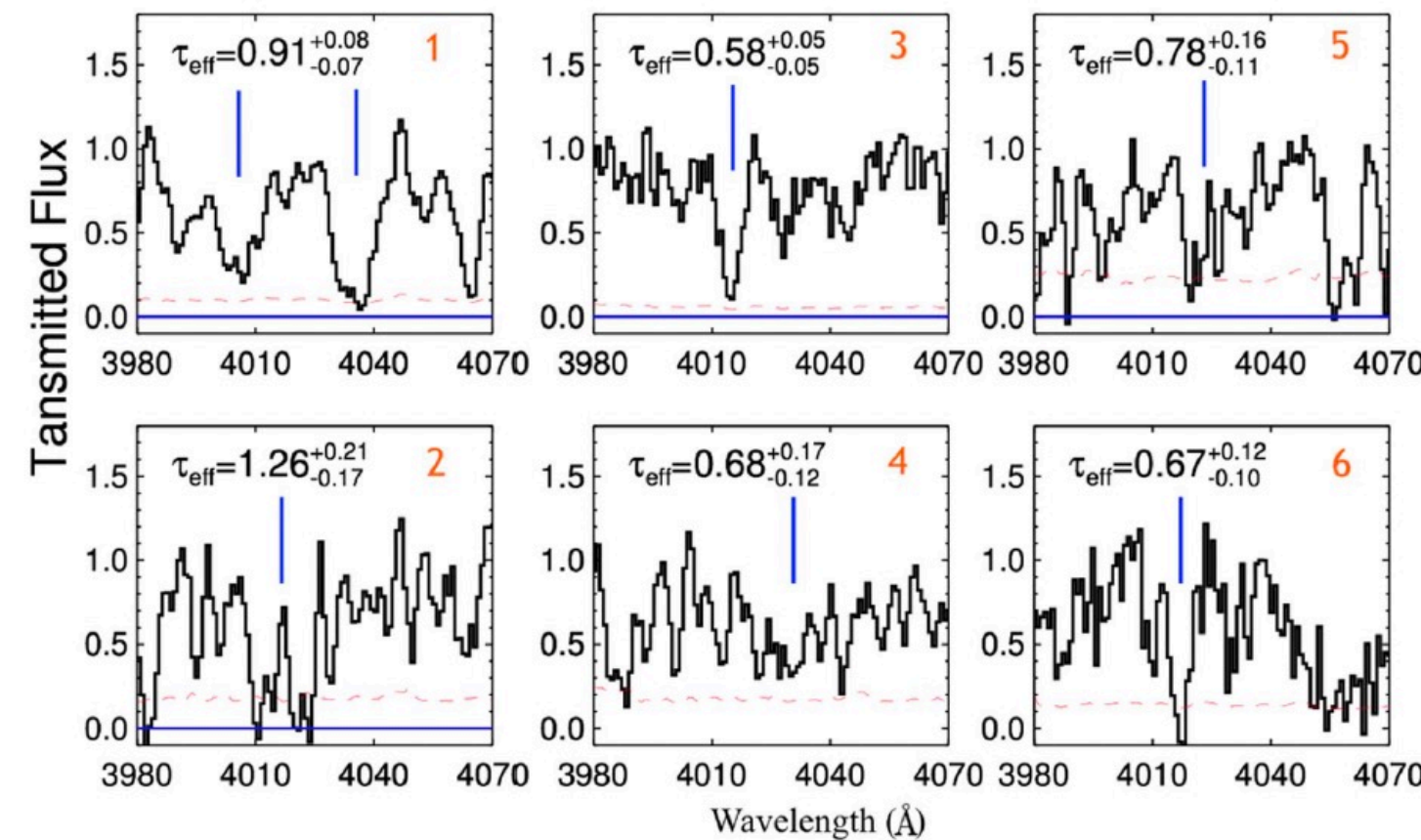


Alexander & Hickox (2012)



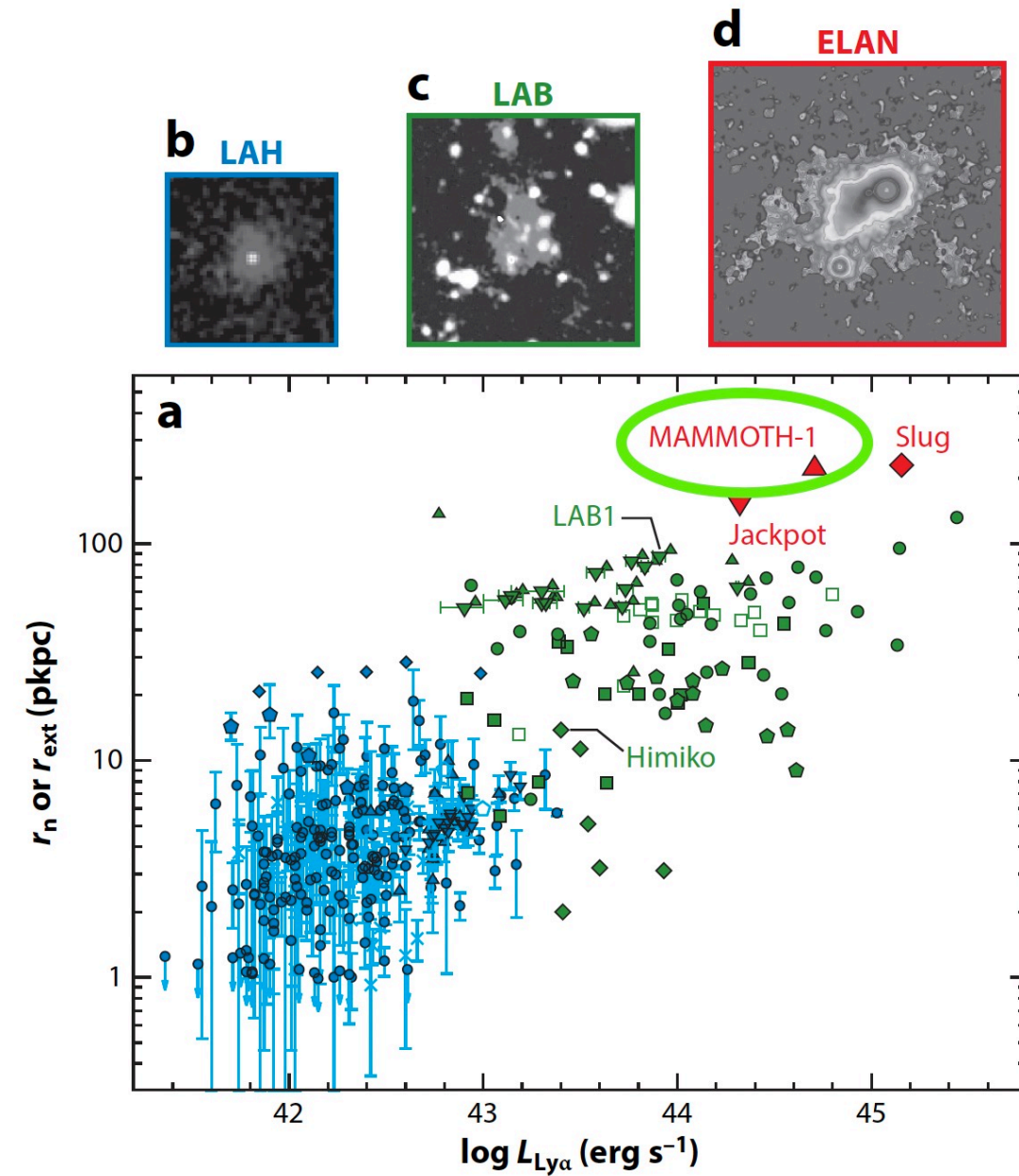
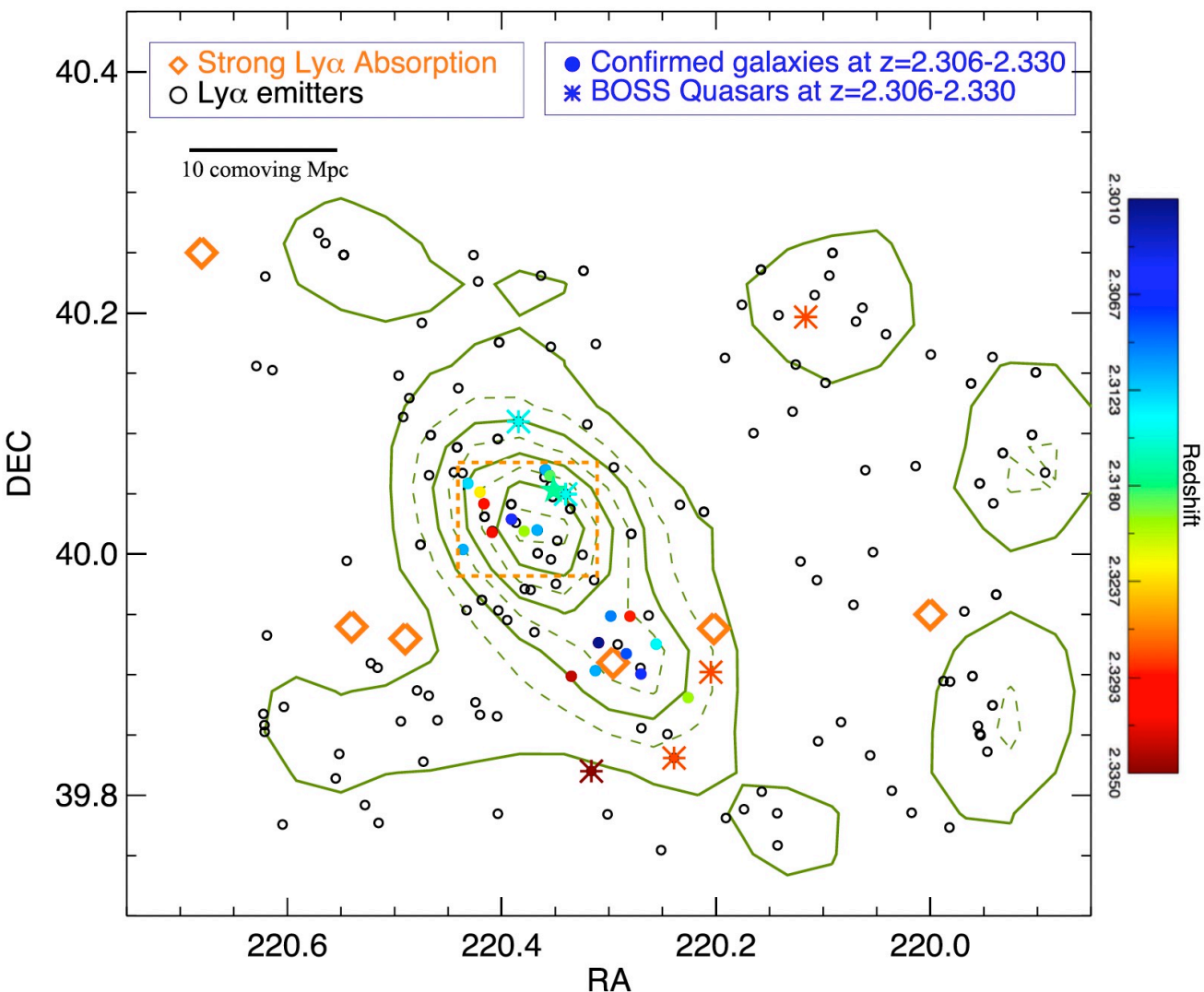
Mapping the Most Massive Overdensities through Hydrogen (MAMMOTH)

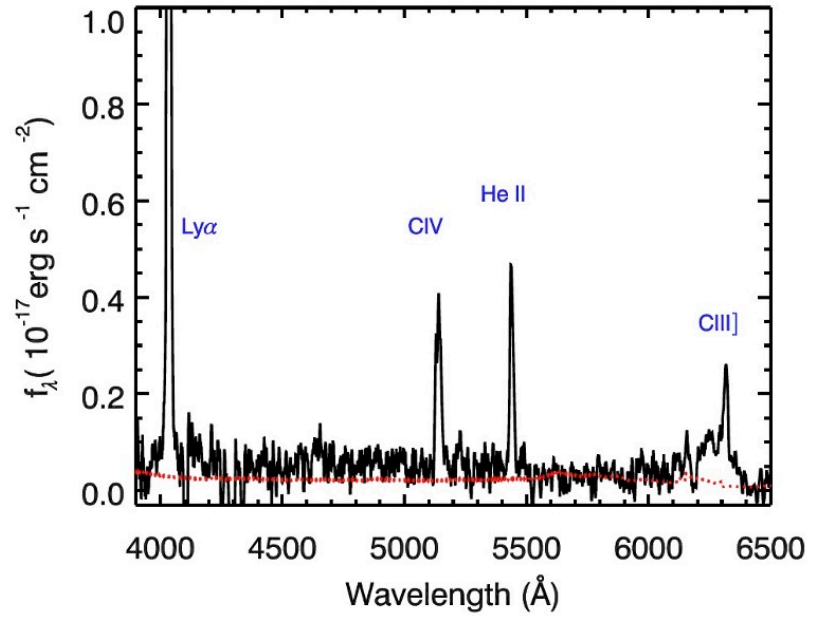
Cai et al. (2016)



Systematic search from BOSS
 ≥ 4 IGM absorbers within 20 Mpc
11 overdensities at $z = 2.32 \pm 0.02$
follow-up with NB403 on KPNO (4m)

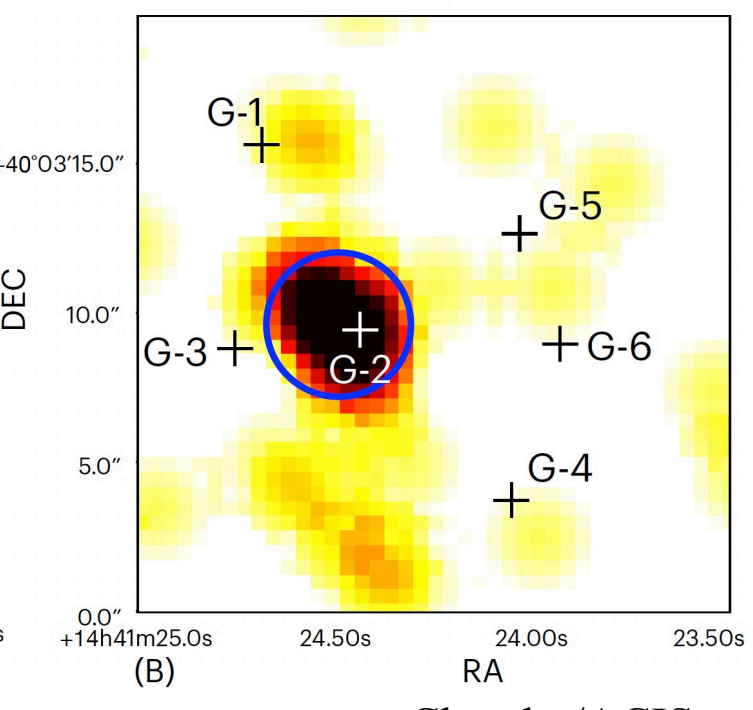
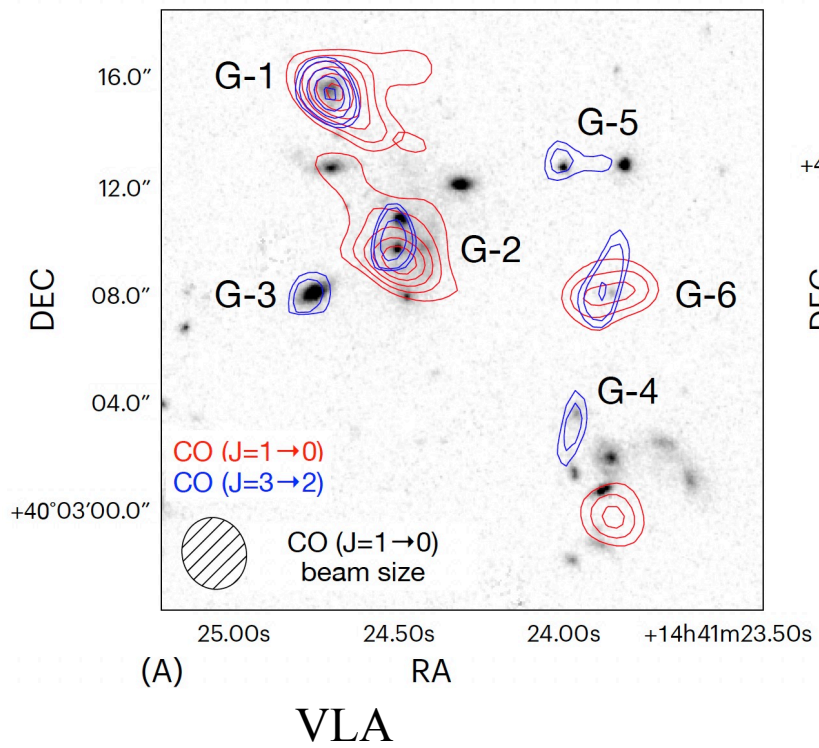
MAMMOTH-1 in BOSS1441 enormous Ly α nebula (ELAN)



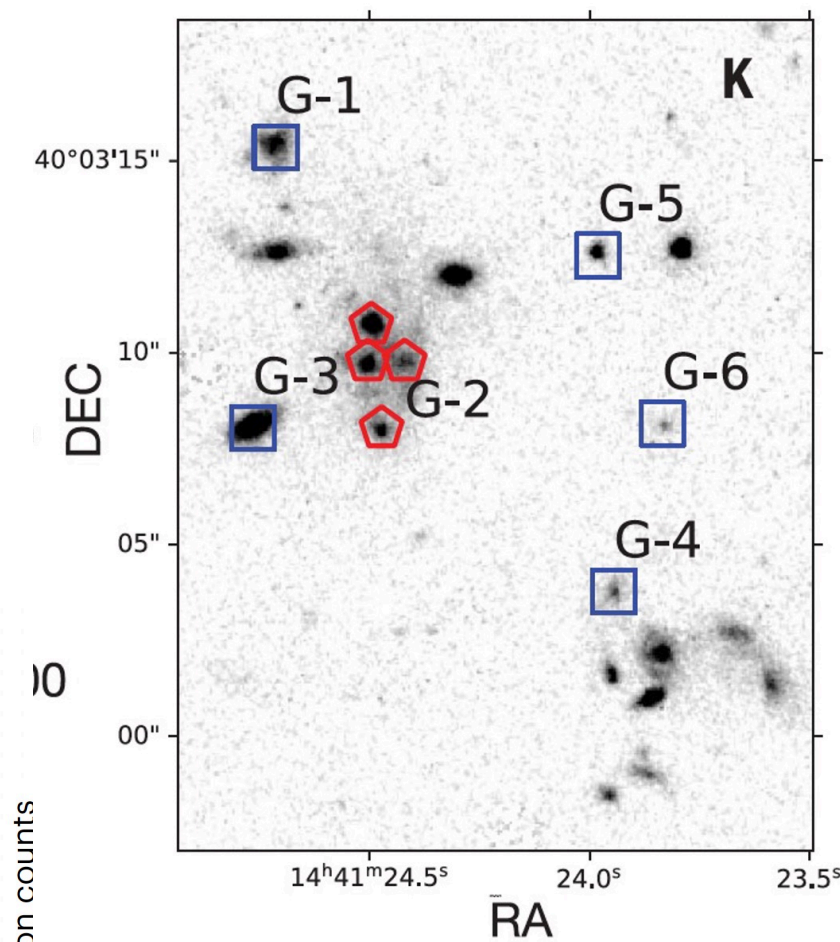


Cai et al. (2017a)

LBT (8m)
longslit

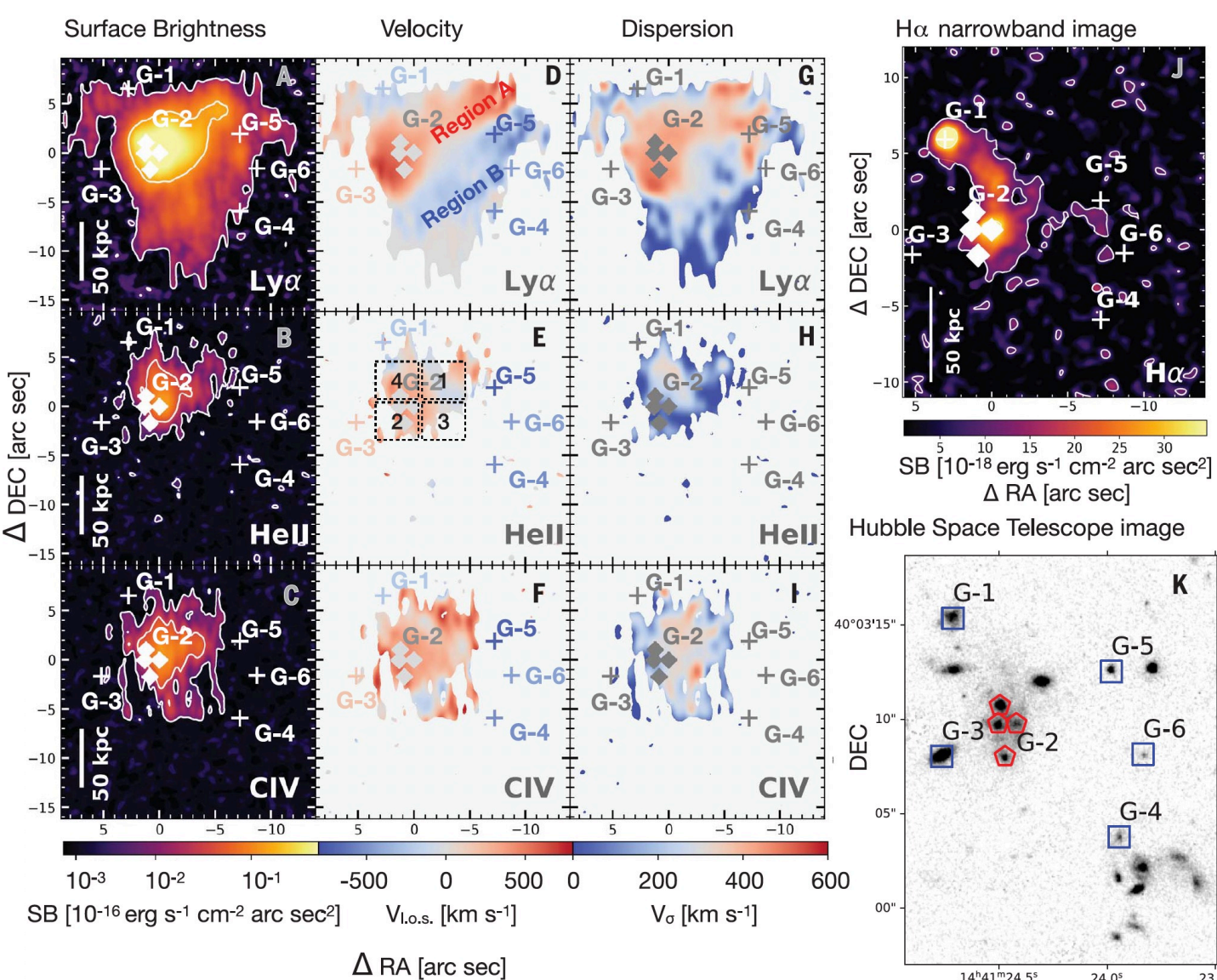
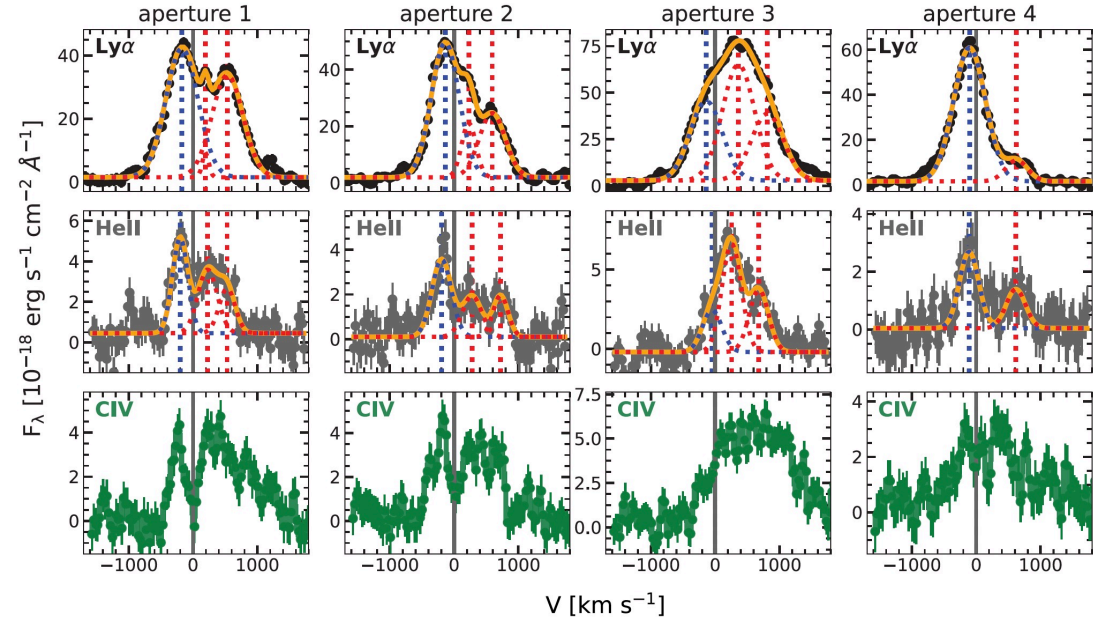


Hubble Space Telescope image



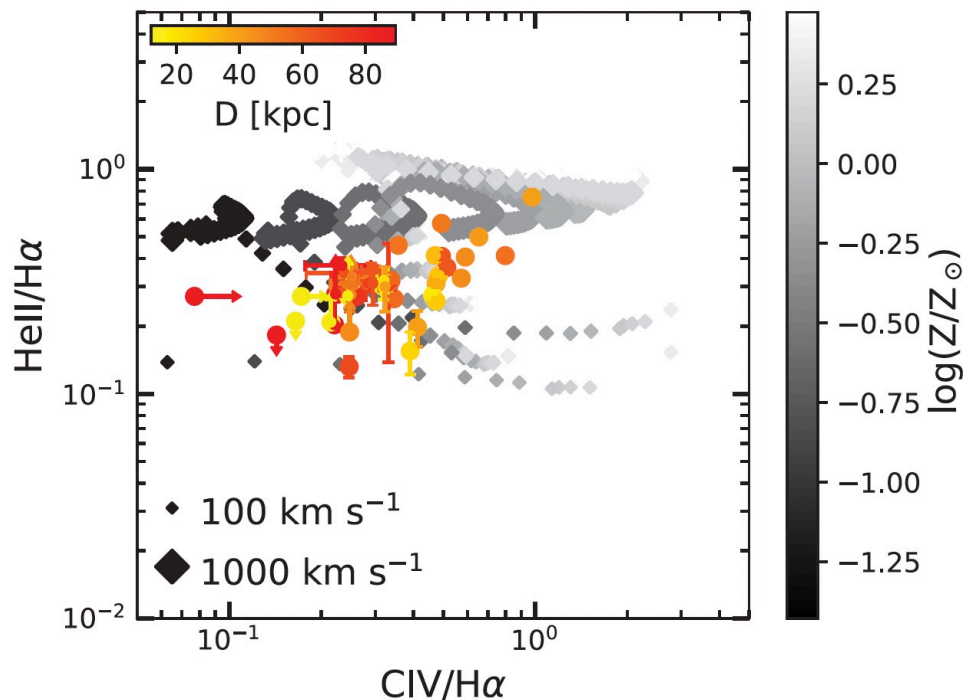
Emonts, Z.C., et al., (2019), ApJ, 887, 86
Li, ..., Z.C., et al., (2021), 922, 236

Our team observed MAMMOTH-1 with the Keck Cosmic Web Imager (KCWI) on the 10-m Keck II telescope in imaging spectroscopy mode centered on the Ly α , C IV 1548/1550 Å, and He II 1640 Å emission lines. We also performed narrowband imaging of redshifted H α (another line of neutral hydrogen with a rest-frame wavelength of 6563 Å) emission using the Multi-Object InfraRed Camera and Spectrograph (MOIRCS) on the 8-m Subaru telescope of multiple Gaussians. The Ly α and He II emission spectra have similar double- or triple-peaked profiles at each location, indicating that the line profiles are attributable to the motion of the ionized gas rather than Ly α radiative transfer effects (17). Using smaller



origin of the diffuse ionized gas
- physical mechanism
- spatial origin

line ratio => emission mechanism => pure photoionization ✗
shock-with-precursor ✓



MAPPINGS III

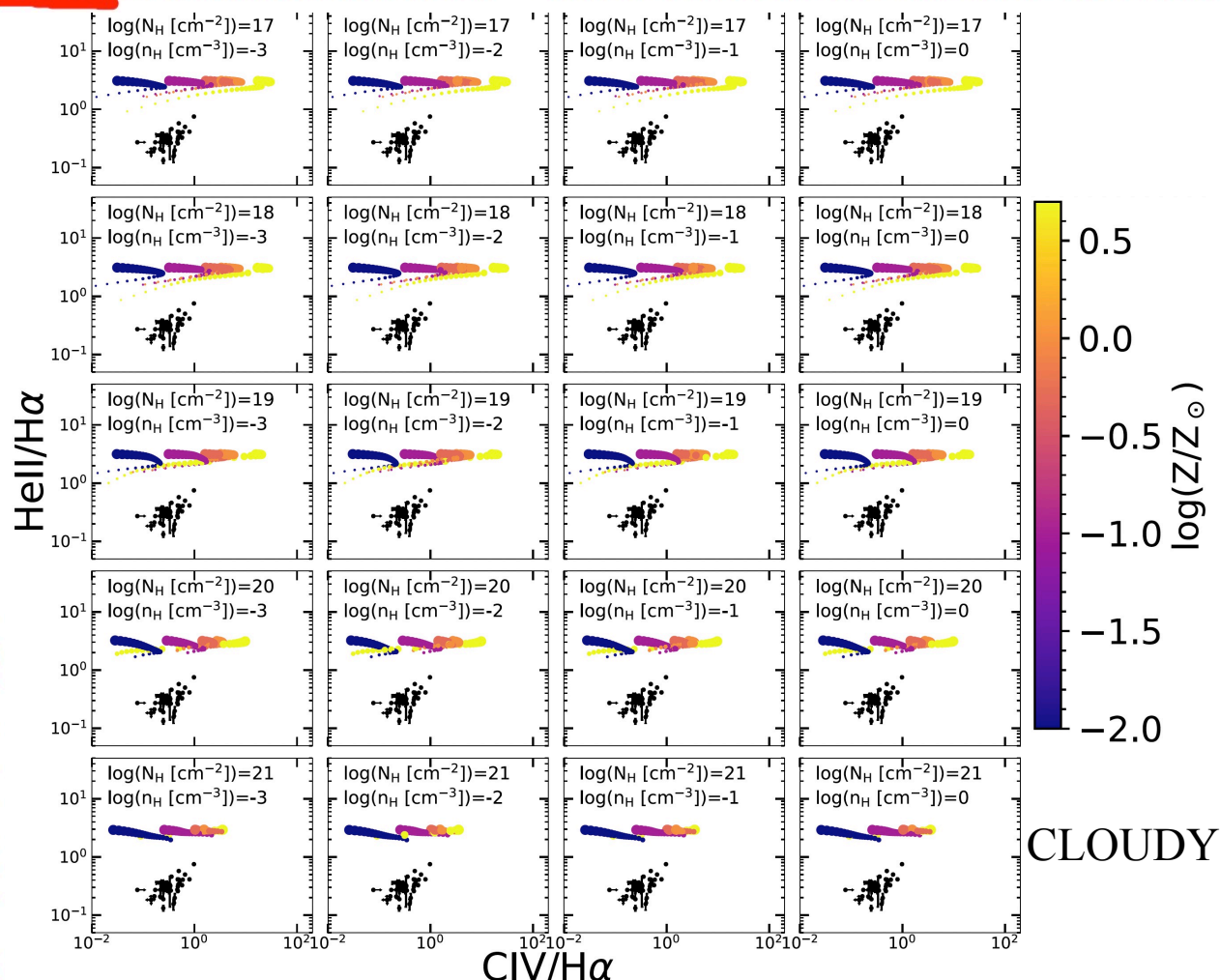
affected by dust attenuation; we estimate that the potential effect of dust on the line ratios is <15% (15). We consider two possible emission mechanisms: In the pure photoionization scenario, the gas is highly ionized by strong ultraviolet radiation from the quasar, causing the line emission to be dominated by recombination. In the alternative shock-with-precursor scenario, the gas moves at a velocity higher than the local sound speed, so a shock front forms at the leading edges of the clouds. Such

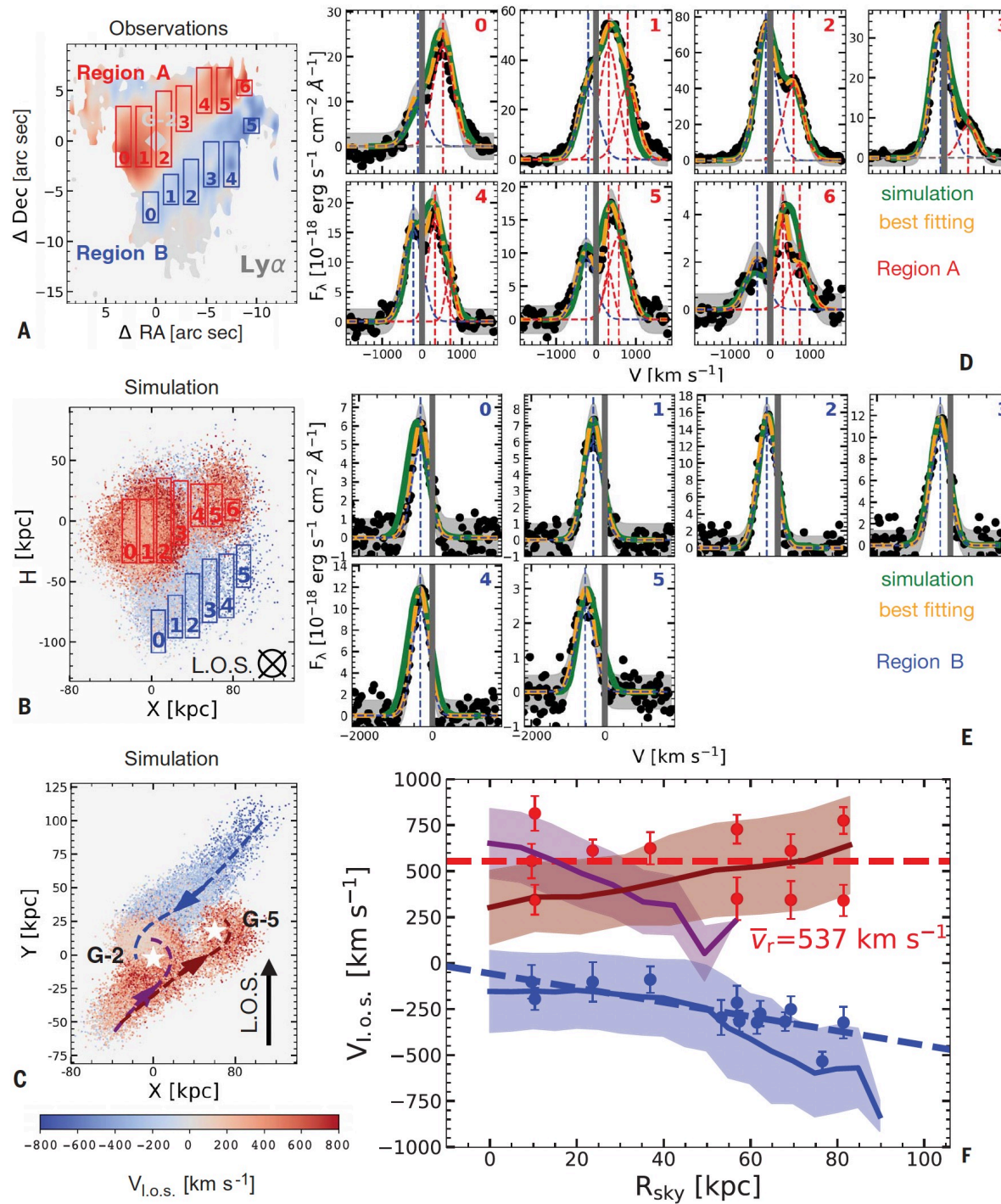
shocks could heat the gas to sufficiently high temperatures that it cools by emitting soft x-rays (19). Model line ratios are shown in fig. S5 for the pure photoionization scenario and in Fig. 3 for the shock-with-precursor scenario. The observed C IV/Hα ratio is consistent with both scenarios, whereas the He II/Hα ratio can only be produced by the shock-with-precursor scenario—it is an order of magnitude smaller than predicted for the pure photoionization model. We examined alternative assumptions

mechanism responsible for the observed emission line.

From the line ratio diagnostics, we find that the CGM metallicities are within 2σ of the solar metallicity (Z_\odot) (Fig. 3). This is an order

of magnitude higher than previous measurements of the metallicity of the interstellar medium in other galaxies with a stellar mass, M_* , of $\leq 10^9 M_\odot$ at $z \approx 2$ to 3 (20, 21) but consistent within 2σ with the CGM metallicity





AGN outflow ✗
Inspiring stream ✓

pect any outflow to decelerate as it propagates into the CGM, as a result of energy loss (25–27). Instead, the observed line-of-sight velocity profile (Fig. 4F) shows that the redshifted velocity is roughly constant and that the absolute value of the blueshifted velocity increases with in-

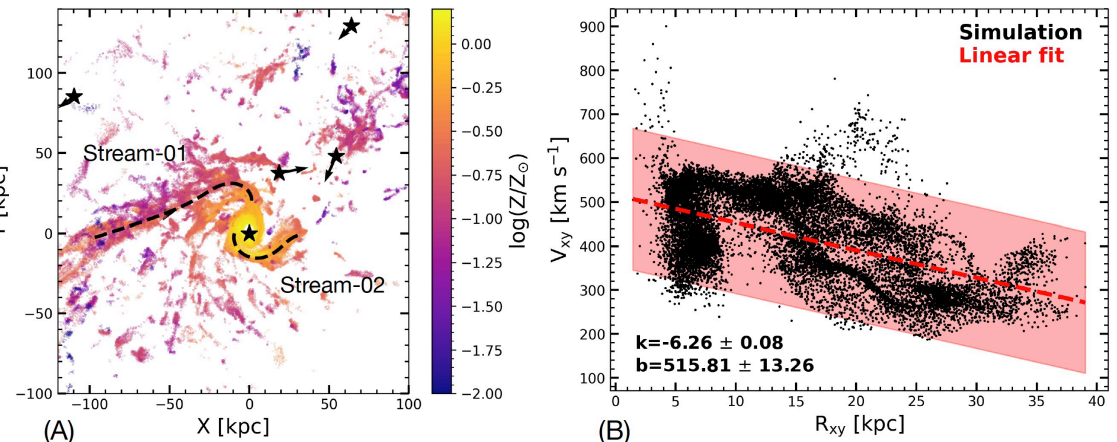


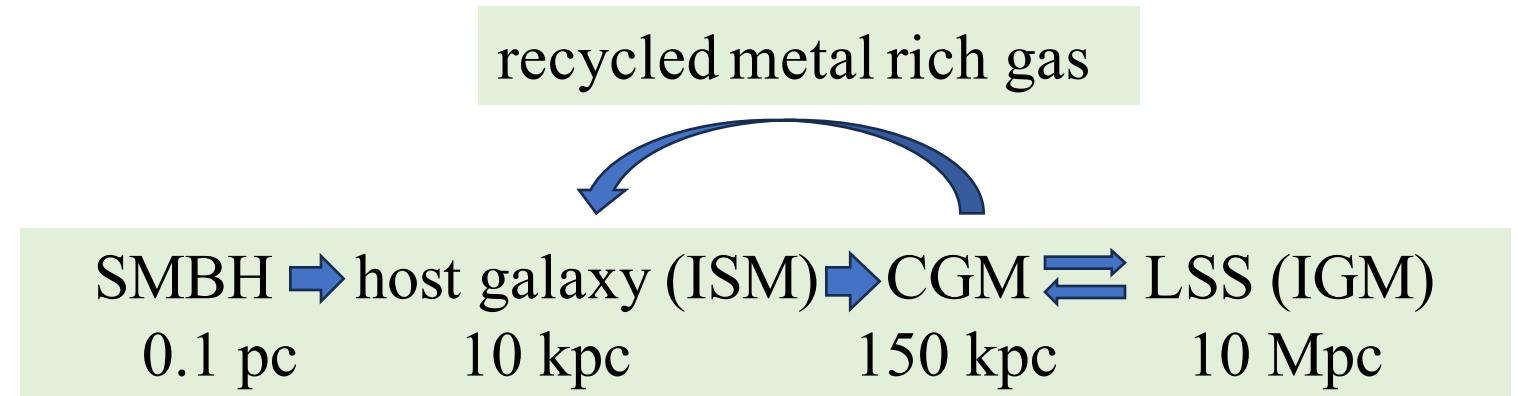
Figure S8: Example of cool gas kinematics in simulations. (A): A simulated system taken from the TNG-100 box (29), which has similar properties to MAMMOTH-1. The color encodes the metallicity. The cool gas ranges from a few tenths to one solar metallicity (Z_\odot) on the scale of 100 kpc, consistent with our observations. Black stars mark the halos in this system. Two major inspiraling streams were fitted using Eq. S11 (black dashed lines). (B): The velocity profile of stream-02 in panel A. Black dots represent the gas particles from simulations, the red dashed line is a linear model fitted to the points, and the red box denotes the 2- σ scatter.

Cosmological simulations have also shown that recycled inflows can provide gas accretion at $z \sim 0$ (8, 9). Other simulations (7) have shown

that, at $z = 2$, the fraction of stellar mass contributed by recycled gas is 40% in a $10^{12.8} M_\odot$ halo. Our interpretation of the MAMMOTH-1 observations is consistent with the latter scenario (7). FIRE

We calculate that the streams provide a mass inflow rate $\dot{M}_{\text{in}} = 703_{-78}^{+101} M_\odot \text{ year}^{-1}$ (15), which is higher than the SFR of G-2 ($81 \pm 18 M_\odot \text{ year}^{-1}$) derived from its far-infrared emission (15). We

with the CGM angular momentum. Any satellite galaxies moving around G-2 could impart angular momentum to the enriched cool CGM gas, which would then flow back to the galaxy in an inspiraling stream (fig. S8A). The CGM



Source	CO (J=3→2)				
	Redshift	FWHM [km s ⁻¹]	L [10 ¹⁰ K km s ⁻¹ pc ⁻²]	v [km s ⁻¹]	M_{H_2} [10 ¹⁰ M_\odot]
G-1	2.3088 ± 0.0004	184 ± 32	7.1 ± 1.1	-253 ± 51	4.3 ± 0.1
G-2	2.3120 ± 0.0006	370 ± 91	6.7 ± 1.4	0 ± 51	4.0 ± 0.1
G-3	2.3137 ± 0.0004	181 ± 75	3.0 ± 1.1	190 ± 51	2.1 ± 0.8
G-4	2.3059 ± 0.0004	161 ± 47	3.7 ± 0.9	-516 ± 51	2.6 ± 0.6
G-5	2.3037 ± 0.0003	81 ± 28	2.1 ± 0.6	-715 ± 45	1.5 ± 0.4
G-6	2.3067 ± 0.0005	281 ± 74	5.4 ± 1.2	-443 ± 57	3.6 ± 0.1

